

Positioning planning of high-intensity-focused ultrasound surgery platform using Bezier curve

Xiang Linqing Ma Peisun Xu Jianbo Gao Xueguan

(Institute of Robotics, Shanghai Jiaotong University, Shanghai 200030, China)

Abstract: A positioning volume ellipsoid method is proposed to represent tumor volume in the workspace of a high-intensity-focused ultrasound (HIFU) surgery platform during the platform's positioning motion. To this simplified tumor model a nearest neighbor search method is used to determine intermediate configuration and goal configuration, which the treatment head and ultrasound focus must pass in their localization to target volume. Based on the decided configurations, the continuity condition of combined Bezier curve in Euclidean space and De Casteljau algorithm on Lie group $SO(3)$ are integrated to construct a combined Bezier positioning path of C^2 continuity at junctional configuration, and an illustration of different positioning path planning is analyzed in detail based on a liver tumor case.

Key words: positioning planning; workspace; key configuration; high-intensity-focused ultrasound (HIFU); Bezier curve; continuity

High-intensity-focused ultrasound (HIFU) surgery platform is a kind of positioning and operation device in ultrasound surgery application. The research on the platform application includes two main topics. One is mainly concerned with the mechanism of action between human tissue and ultrasound focus, and this includes pressure field and temperature field distribution and evolvment in the tissue^[1]. The other is concentrated on the device application, and the primary coverage is how to use sophisticated automation technology, robotics theory and graphics algorithms to solve problems in the practical application of the platform, for example the solution of the positioning planning and therapy planning problem^[2].

Positioning planning aims to construct a positioning path in the workspace, such that by moving along this path, it is possible for the ultrasonic focus to be located at the tumor nidus. This path construction task can be described as determining several key configurations $\{O_i; x_i, y_i, z_i, \alpha_i, \beta_i, \gamma_i, i = 1, 2, \dots, m\}$ in the workspace, then interpolation or approximation of the solved configurations is applied to achieve a general configuration transformation of ultrasound focus during the positioning motion. In our opinion this is a path-planning problem in the workspace of a specific robot. In general there are two methods to solve a robot path

planning problem in task space. One is to use an optimization method and polynomial curve to find a optimal path to some special objectives^[3], but this type of method requires complex computation, which is not suitable for planning online. The other way to find the path in the workspace is by employing the spline to path planning, such as B-spline or Bezier spline^[4]. This method is not the optimized result of some objective energy function, which has specific physical meaning, but the calculation of this method is more efficient than the previous one, and can be completed in real time. Then tracking of the planned path is also easy to realize. In this paper we achieve a positioning path of C^2 continuity at junctional configuration to our developed HIFU surgery platform by determining the workspace, configuring proper intermediate and ultimate goals and then by interpolating the defined configuration using a combined Bezier curve in Lie group $SE(3)$.

1 Structure and workspace of the HIFU surgery platform

The structure of the HIFU surgery platform is diagramed in Fig.1. The functional components of the platform include C arm, a three-coordinate bed and an internal motion subsystem in the treatment head. According to Ref. [5], a multiple-robot cooperating system is suitable for modeling kinematics of such a positioning system; consequently, the positioning system is viewed as a two-robot cooperating system, which consists of a five-degree of freedom robot (C arm and internal motion subsystem) and a three-degree of freedom robot (three-coordinate bed). These

Received 2003-10-14.

Foundation item: The Developing Foundation of Shanghai Science and Technology Committee (No. 994419027).

Biographies: Xiang Linqing (1974—), male, graduate; Ma Peisun (corresponding author), male, professor, psma@sjtu.edu.cn.

two robots manipulate the patient's body, but each has its own working motion process, moreover, these two robots can be in different configuration status during the positioning procedure and in the terminal positioning situation, so in nature the two-robot cooperating system is a loose cooperating system described in Ref.[6]. According to the description of the loose cooperating robot system, this kind of cooperating system is modeled as an open chain robot system at last, so is the surgery platform.

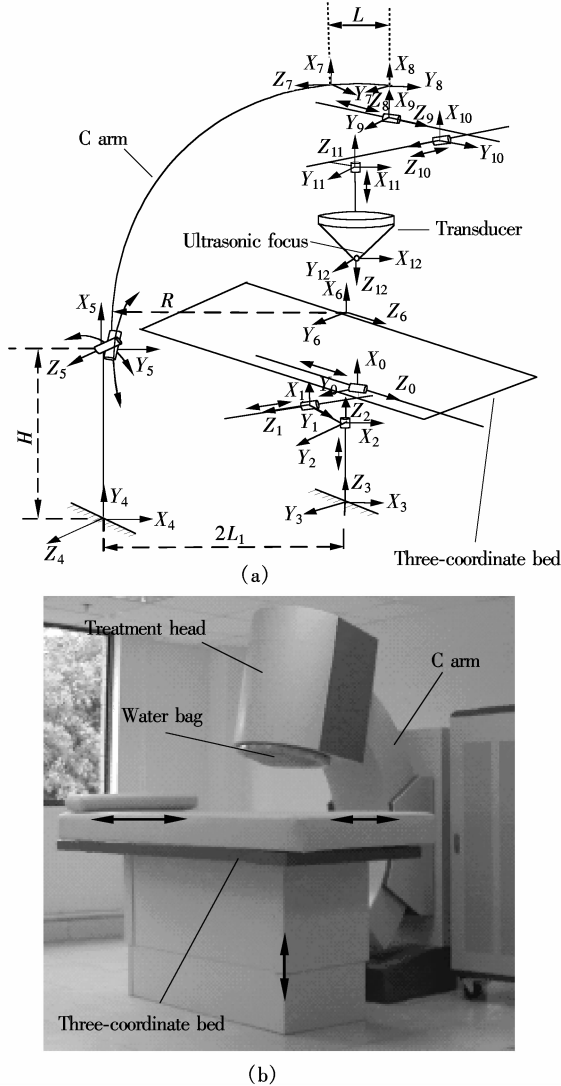


Fig.1 Structure of the HIFU surgery platform and its coordinate system. (a) Schematic diagram of the HIFU surgery platform and its coordinate system; (b) HIFU surgery platform overview

The most direct way to describe the positioning course of the ultrasound focus is using relative configuration transformation of the ultrasound focus and the treatment head with respect to the three-coordinate bed; thus the coordinate system $X_0Y_0Z_0$ is attached to the bed when formulating the positioning motion; all the other coordinate systems are set up with respect to the $X_0Y_0Z_0$ system. The established

coordinate systems are shown in Fig.1, and in this coordinate system the Denavit-Hartenberg parameters of the surgery platform are given, and the kinematics equation of the motion system is also formulated as

$$g_s(\theta) = \begin{bmatrix} -c\theta_8s\theta_5 & -s\theta_4 & -c\theta_5c\theta_5 & hc\theta_5c\theta_5 - Rc\theta_5c\theta_5 + H + d_3 - d_5c\theta_5s\theta_5 + d_7s\theta_4 - (d_8+f)c\theta_5c\theta_5 \\ -c\theta_5 & 0 & s\theta_5 & R s\theta_5 + 2L_1 + d_2 - R - Lc\theta_5 - hs\theta_5 - d_5c\theta_5 + (d_8+f)s\theta_5 \\ -s\theta_5c\theta_5 & c\theta_4 & -s\theta_5c\theta_5 & hs\theta_5 - R s\theta_5c\theta_5 + d_1 - Ls\theta_5s\theta_5 - d_7c\theta_4 - (d_8+f)s\theta_5c\theta_5 \\ 0 & 0 & 0 & 1 \end{bmatrix} g(0) \quad (1)$$

where $H = 690$ mm, $h = 8.5$ mm, $L_1 = 505$ mm, $L = 278$ mm, $R = 790$ mm, $c\theta_i$ represents $\cos\theta_i$ and $s\theta_i$ represents $\sin\theta_i$, and $g(0)$ is the initial configuration of the ultrasound focus. The computation result of the workspace is presented in Fig.2. According to Fig.2 it is concluded that the workspace of the platform is wide enough for most surgical operations on a patient's organs. When the patient takes supine position and prone position in the positioning and surgery, the ultrasound focus can catch all the organs in the patient's chest, abdomen and pelvis. As the lateral position and seated position are also taken as treatment postures, all the organs of the patient can be focused on by ultrasound, and the tumor in the focalized organ can be ablated.

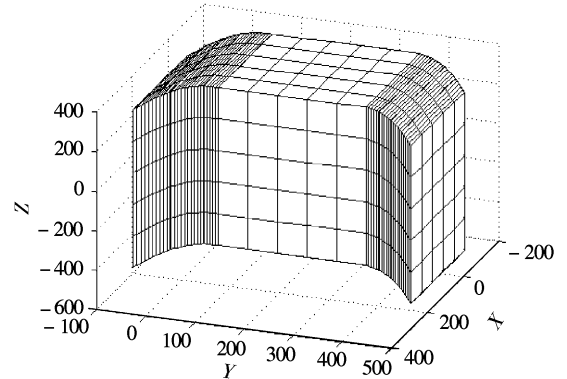


Fig.2 Workspace analysis result of HIFU surgery platform

2 Key Configuration Determination of the Positioning Path Planning

2.1 Brief introduction to the positioning procedure

When positioning, the treatment head moves in the workspace of the platform. In the movement the water bag (indicated in Fig.1.) in the front of the treatment head firstly contacts with patient's body, and all the subsequent positioning movement aims at locating the ultrasound focus inside the tumor volume. The ultrasound transducer does not work during positioning, so it is assumed that the ultrasonic transducer work and a virtual ultrasound focus will generate; based on analysis of the shape of the ultrasonic focus in Ref. [1] and our transducer parameters, the generated virtual ultrasound focus can be viewed as a $10 \text{ mm} \times 3 \text{ mm} \times 3 \text{ mm}$ ellipsoid, and

the mathematical equation of the ellipsoid is

$$E_{\text{focus}} : f(x, y, z) = \frac{x^2}{a^2} + \frac{y^2}{b^2} + \frac{z^2}{c^2} - 1 = 0$$

$$a = 10, b = c = 3$$

In the positioning procedure this virtual focus acts as a special heating end effector, and this special end effector is attached to the treatment head, which moves and yields rigid motion in workspace until it reaches the target tumor region.

2.2 Simplified representation of tumor volume in workspace

The shape of the tumor is extremely irregular; so only the position and posture of the tumor volume are essential for the positioning process, so in determining of the positioning path configuration a positioning volume ellipsoid method is proposed to model the tumor's location and orientation in the platform workspace. The positioning volume ellipsoid is determined by tumor point set, the tumor contour points are distributed inside the ellipsoid or on the ellipsoid surface, and the center of the positioning volume ellipsoid C is also derived from the tumor point set.

Definition 1 The positioning volume ellipsoid is the smallest ellipsoid E in workspace, the tumor contour points are distributed inside the ellipsoid or on the ellipsoid surface, the center of the positioning volume ellipsoid C can also be derived from the tumor point set, so for all elements in point set, the following equation of the positioning volume ellipsoid must be satisfied:

$$\{E: (X - C)^T Q (X - C) \leq 1 \mid S \subseteq E, X \in \mathbf{R}^3, C \in \mathbf{R}^3, Q = AA^T\} \quad (2)$$

where $Q = AA^T$ is a positive symmetric matrix, AA^T is Cholesky decomposition of matrix Q , and $X \in \mathbf{R}^3$ is coordinate value of the tumor point. Calling for eigenvalue decomposition of Q leads to

$$M = \begin{bmatrix} \lambda_1 & & \\ & \lambda_2 & \\ & & \lambda_3 \end{bmatrix} = \tilde{P}^{-1} Q \tilde{P} \quad (3)$$

where $\lambda_1, \lambda_2, \lambda_3$ are three eigenvalues of Q . For the description of the tumor, these three eigenvalues are set as the length of three axes of the positioning volume ellipsoid, after normalization, the column vectors of the matrix \tilde{P} are used to represent orientation of the ellipsoid's three axes, thus the body of the positioning volume ellipsoid denotes the position occupation and rough shape of the tumor, and the three axes of the positioning volume ellipsoid indicate the round posture of the tumor.

To solve the positioning volume ellipsoid

problem, a weight $\omega_i (i = 1, 2, \dots, n)$ is set to every point in the tumor point set $P = \{(X_i, Y_i, Z_i) \mid X_i \in \mathbf{R}, Y_i \in \mathbf{R}, Z_i \in \mathbf{R}, i = 1, 2, \dots, n\}$ obtained from image processing, so the whole point set can be represented by new expression $P^* = \{(\Omega, (X_i, Y_i, Z_i)) \mid \Omega \in \mathbf{R}, X_i \in \mathbf{R}, Y_i \in \mathbf{R}, Z_i \in \mathbf{R}, i = 1, 2, \dots, n\}$. The weight value is assigned according to the convex hull of the point set P . When the point is located on the convex hull the weight is adopted as $\omega_i = 1$, while to all the other points the weight value satisfy $\omega_i < 1$, in the application these weight, span is 0.5 to 0.9. To the whole point set, a covariance matrix \tilde{M} can be constructed as

$$\tilde{M} = \begin{bmatrix} V(X) & C(X, Y) & C(X, Z) \\ C(Y, X) & V(Y) & C(Y, Z) \\ C(Z, X) & C(Z, Y) & V(Z) \end{bmatrix} \quad (4)$$

where $C(X, Y) = E(XY) - E(X)E(Y) = C(Y, X)$ is the covariance of the X, Y coordinates, $XY = \{X_1 Y_1, \dots, X_n Y_n\}$, $E(X) = \sum_{i=1}^n (w_i X_i) / \sum_{i=1}^n w_i$ and $E(Y)$, $E(Z)$ are mathematical expectations of point set's coordinate values. The variance of X coordinate is $V(X) = E(X - E(X))^2$, and all the other elements of the covariance matrix \tilde{M} can be obtained by applying the same covariance and variance definition to other coordinates of the tumor point set. In general the covariance matrix is a positive symmetric matrix, the eigenvalues of matrix \tilde{M} satisfy $\tilde{\lambda}_1 \geq \tilde{\lambda}_2 \geq \tilde{\lambda}_3 > 0$, an orthogonal coordinate system can also be obtained from the corresponding normalized eigenvectors of \tilde{M} , so if $\{E(X), E(Y), E(Z)\}$ is employed as the center of ellipsoid C and matrix \tilde{M} is adopted as ellipsoid matrix M , a positioning volume ellipsoid $E = (P - C)^T \tilde{M} (P - C) \leq 1$ to represent the tumor location and orientation is constructed.

2.3 Determination of key configurations in positioning motion

At the beginning of the positioning procedure, all parts of the platform are in their initial states, so the starting configuration of the treatment head can be calculated from the geometry relationship between concerning reference coordinate systems. To the goal positioning configuration of the treatment head and ultrasound focus ellipsoid, the position of the goal configuration is determined firstly. By introduction of the positioning volume ellipsoid, the positioning procedure is re-described as follows: to any finished positioning procedures only when the virtual ultrasound focus is located inside the positioning

volume ellipsoid at the end of positioning motion, the positioning procedure is considered as an effective positioning course, and the closer the focus ellipsoid is to the center of the positioning volume ellipsoid, the more accurate the whole positioning procedure is, so it is reasonable to take $C = \{E(X), E(Y), E(Z)\}$ as the goal position of the positioning.

The goal pose of the treatment head and ultrasound focus ellipsoid are settled by the incident angle of ultrasound after the ultrasound is focused on the target tumor volume. Considering ultrasound propagation, in order that the ultrasound energy loss is minimal during its propagation in the patient's body, the ultrasound propagation path must be the shortest way when the ultrasound beam enters the patient's body from the ultrasound transducer located outside the body at the goal configuration. The shortest propagation path is the line path which links a point in body surface contour point set to the goal position C , and the point must be the nearest point of C , so the goal pose problem can be uniquely determined by finding out the nearest neighbor point to C under the Euclidean norm L_2 in a specific point set. The specific point set is determined by limit of the joint parameter of the platform's C arm. It consists of all patient's body surface points enclosed by a symmetric tetrahedron. The tetrahedron takes C as a vertex and the vertical line passing C as the height line and symmetry axis, the angle between the height line and each side plane is either 15° or 20° . For this specific point set $P = \{p_j \in \mathbf{R}^3\} (j = 1, 2, \dots, m)$ and the center of positioning volume ellipsoid C , a nearest neighbor search is applied to find out the nearest neighbor point of the center of positioning volume ellipsoid, which satisfies $p_k \in P, \|C - p_k\| \leq \|C - p_j\|, \forall p_j \in P$. The result line $p_k C$ connecting these two points is the incident axis of the ultrasound focus at the end of the positioning, and the angle between the resulted incident line and the three axes of the $X_0Y_0Z_0$ coordinate system is used as the goal pose of the treatment head. There are a lot of methods to solve the nearest neighbor query problem of the point set, and the method given in Ref. [7] is used in this paper.

In order to guarantee the accuracy of the terminal positioning configuration for the positioning motion, the successful and precise localization to the point p_k must be realized before the treatment head and ultrasound focus ellipsoid move to the goal configuration, so the point p_k must be employed as an intermediate path point so that the treatment head and ultrasound focus ellipsoid must pass in the positioning

course; in addition, the treatment head must keep tight contact with the patient's body after positioning is over, so p_k is also used as the beginning contact point with the patient's body surface during positioning. If the orientation of the treatment head changes a lot after touching the patient's body surface, the posture of the patient's body may also change correspondingly, and these changes may result in a positioning error, so it is decided that 80% of the orientation change in the whole positioning motion is realized in the positioning motion from the initial configuration to the intermediate configuration. The intermediate path point p_k and the goal configuration $p_k C$ of the positioning process are shown in Fig.3.

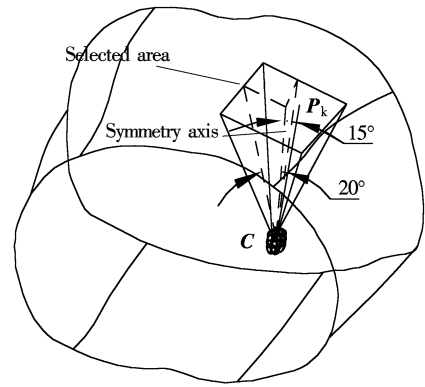


Fig.3 Abdomen contour, positioning final configuration $p_k C$ and intermediate positioning location P_k

3 Positioning Path Planning of the HIFU Surgery Platform

3.1 Description of the positioning path planning^[9]

In order to protect patient from damage, it is required that the planned positioning path has continuously changing velocity and acceleration, and it is also required that the velocity and acceleration decrease gradually as the treatment head approaches the patient's body more and more, so the path must have at least C^2 continuity to easily realize the change of the velocity and acceleration. According to the previous analysis, three path configurations $g_o, g_{mid}, g_f \in SE(3)$ ^[8] can be determined, where g_o is the initial configuration of the treatment head and ultrasound focus ellipsoid, g_{mid} is the intermediate configuration and g_f is the terminal configuration of the positioning motion. When solving the positioning planning problem, it is assumed there is a path $g(t) = \begin{bmatrix} R(t) & p(t) \\ 0 & 1 \end{bmatrix}$, $R(t) \in SO(3)$, $p(t) \in \mathbf{R}^3$, $g(t) \in SE(3)$ in the workspace. By moving along this path, the treatment head and ultrasound focus ellipsoid are

in their initial configuration \mathbf{g}_o at time $t = r$; at $t = v$ the virtual ultrasound focus ellipsoid reaches the tumor volume location and the treatment head also reaches its goal configuration \mathbf{g}_f ; at $t = s$ the virtual ultrasound focus ellipsoid passes the intermediate configuration \mathbf{g}_{mid} , so the path must meet at least the following boundary condition:

$$\begin{aligned} \mathbf{g}(r) &= \mathbf{g}_o, \quad \left. \frac{d\mathbf{g}}{dt} \right|_{t=r} = \dot{\mathbf{g}}_o, \quad \mathbf{g}(v) = \mathbf{g}_f, \\ \left. \frac{d\mathbf{g}}{dt} \right|_{t=v} &= \dot{\mathbf{g}}_f, \quad \mathbf{g}(s) = \mathbf{g}_{\text{mid}} \quad r < s < v \end{aligned} \quad (5)$$

3.2 Solution to the Bezier positioning path

Unlike planning the positioning path using the polynomial curve^[3], which results in a complex optimization problem, the Bezier curve path^[4] can be gained by determination of the control polygon, and all vertices of the control polygon are obtained from computation of the known boundary condition, so it is advantageous to apply the Bezier curve to describe the platform planning positioning path. In Ref. [4], a detailed description of the De Casteljau algorithm used to construct the Bezier curve connected two points in SO(3) group is given, based on the Bezier curve theory and algorithm, the continuity condition of the combined Bezier curve in Euclidean space^[9] is extended to SE(3) in this paper to design a combined Bezier curve positioning path; firstly application parameterization to two intervals $[r, s]$, $[s, v]$, which is given in the previous subpart, leads to

$$\begin{aligned} t_1 &= \frac{t-r}{s-r}s + \left(1 - \frac{t-r}{s-r}\right)r \quad r < t < v, 0 \leq t_1 \leq 1 \\ t_2 &= \frac{t-r}{s-r}v + \left(1 - \frac{t-r}{s-r}\right)s \quad r < t < v, 0 \leq t_2 \leq 1 \end{aligned}$$

To these two parameters t_1 , t_2 , two segments of Bezier curve $\mathbf{P}(t_1)$, $\mathbf{Q}(t_2)$ can be designed to interpolate three path configurations, and the C^2 continuity condition at the junctional path point of $\mathbf{P}(t_1)$ and $\mathbf{Q}(t_2)$ is $\mathbf{P}'(1) = \mathbf{Q}'(0)$.

In these two Bezier curve segments, the motion of $\mathbf{Q}(t_2)$, which connects two path configurations \mathbf{g}_{mid} and \mathbf{g}_f , occurs after the treatment head contacted with the patient's body, so that when the goal configuration is achieved, the velocity and acceleration of the locomotion at this configuration must be zero; accordingly the boundary condition of the $\mathbf{Q}(t_2)$ at configuration $\mathbf{Q}(1) = \mathbf{g}_f$ can be set as $\mathbf{Q}'(1) = 0$, $\mathbf{Q}''(1) = 0$. The first derivative of the intermediate configuration \mathbf{g}_{mid} can be settled by the following assumptions: firstly it is assumed that there exists a uniform motion curve between \mathbf{g}_o and \mathbf{g}_{mid} , and then Eq.(6) must be held, where $\mathbf{V}_{\text{uniform}}^1$ is the velocity

of the uniform motion:

$$\mathbf{g}_{\text{mid}} = \mathbf{g}_o \exp(\mathbf{V}_{\text{uniform}}^1) \quad (6)$$

Application of matrix transformation and a logarithm map to Eq.(6) results in $\mathbf{V}_{\text{uniform}}^1 = \log(\mathbf{g}_o^{-1} \mathbf{g}_{\text{mid}})$; the same procedure can also be used to the uniform motion curve connecting intermediate configuration \mathbf{g}_{mid} and terminal configuration \mathbf{g}_f , which is supposed to exist during interval t_2 , consequently the equations $\mathbf{g}_f = \mathbf{g}_{\text{mid}} \exp(\mathbf{V}_{\text{uniform}}^2)$ and $\mathbf{V}_{\text{uniform}}^2 = \log(\mathbf{g}_{\text{mid}}^{-1} \mathbf{g}_f)$ can be got, where $\mathbf{V}_{\text{uniform}}^2$ is also the speed of the present uniform motion curve. If these uniform motion curves are used to connect three path configurations, two velocities may occur and the resulting path just has C^0 continuity at the intermediate configuration; so in order to achieve a smooth transition in the intermediate configuration, $\mathbf{Q}'(0) = \frac{\mathbf{V}_{\text{uniform}}^1 + \mathbf{V}_{\text{uniform}}^2}{2}$

can be employed as the first order derivative of the intermediate configuration when designing the C^2 continuous combined Bezier curve positioning path. As the interpolating boundary condition $\mathbf{P}(1) = \mathbf{Q}(0) = \mathbf{g}_{\text{mid}}$, $\mathbf{Q}(1) = \mathbf{g}_f$ are attached to solve planning problem, five equations can be obtained, and a piece of a four-order Bezier curve path can be determined by simultaneous solution of these five equations; these five equations are formulated as

$$\begin{aligned} \mathbf{Q}(0) &= \mathbf{g}_{\text{mid}}, \quad \mathbf{Q}(1) = \mathbf{g}_f, \\ \left. \frac{d\mathbf{q}}{dt_2} \right|_{(0)} &= \frac{\log(\mathbf{g}_o^{-1} \mathbf{g}_f)}{2}, \quad \left. \frac{d\mathbf{q}}{dt_2} \right|_{(1)} = 0, \\ \left. \frac{d^2\mathbf{q}}{dt_2^2} \right|_{(1)} &= 12\gamma_1 (\mathbf{V}_3^1 - \mathbf{V}_2^1) \mathbf{g}_f = 0 \end{aligned} \quad (7)$$

To Bezier curve connecting the configurations \mathbf{g}_o and \mathbf{g}_{mid} , its second order derivative at \mathbf{g}_{mid} must be determined by solving the Bezier path segment $\mathbf{Q}(t_2)$ in order to guarantee C^2 continuity of a combined Bezier curve path at that configuration; the first order derivative in \mathbf{g}_o is also set as zero; the first order derivative at configuration \mathbf{g}_{mid} is also $\mathbf{P}'(1) = \mathbf{Q}'(0) = \log(\mathbf{g}_o^{-1} \mathbf{g}_f) / 2$ according to continuity condition. As an interpolating boundary condition of $\mathbf{P}(t_1)$ is attached to the problem solution, the curve can be settled, the equation of $\mathbf{P}(t_1)$ is presented as

$$\begin{aligned} \mathbf{P}(0) &= \mathbf{g}_o, \quad \mathbf{P}(1) = \mathbf{g}_{\text{mid}}, \\ \left. \frac{d\mathbf{p}}{dt_1} \right|_{(0)} &= 0, \quad \left. \frac{d\mathbf{p}}{dt_1} \right|_{(1)} = \frac{\log(\mathbf{g}_o^{-1} \mathbf{g}_f)}{2}, \\ \left. \frac{d^2\mathbf{p}}{dt_1^2} \right|_{(1)} &= 12\gamma_0 (\tilde{\mathbf{V}}_1^1 - \tilde{\mathbf{V}}_0^1) \mathbf{g}_{\text{mid}} \end{aligned} \quad (8)$$

where $\left. \frac{d^2\mathbf{p}}{dt_1^2} \right|_{(1)} = \left. \frac{d^2\mathbf{q}}{dt_2^2} \right|_{(0)}$, and γ_0 , γ_1 can be calculated

by using theorem 2.9 in Ref. [4]. According to the previous analysis on combined Bezier curve path, which is C^2 continuous at intermediate configuration, the procedure to solve the problem is given in detail as follows; the C^0 and C^1 combined Bezier curve path can also be obtained by using similar process.

Step 1 Input initial configuration, intermediate configuration and goal configuration \mathbf{g}_o , \mathbf{g}_{mid} , $\mathbf{g}_f \in SE(3)$ for positioning path planning.

Step 2 Input the first order derivative of the Bezier curve path at configuration \mathbf{g}_{mid} and \mathbf{g}_f , and also input the second order derivative at configuration \mathbf{g}_f to construct a Bezier curve \mathbf{Q} connecting \mathbf{g}_{mid} and \mathbf{g}_f .

① By using $\frac{d\mathbf{q}}{dt_2}(0) = \frac{\log(\mathbf{g}_o^{-1} \mathbf{g}_f)}{2} = 4\mathbf{g}_{mid} \mathbf{V}_0^1$, $\mathbf{V}_0^1 = \frac{\mathbf{g}_{mid}^{-1} \log(\mathbf{g}_o^{-1} \mathbf{g}_f)}{8}$ is obtained, and by $\frac{d\mathbf{q}}{dt_2}(1) = \mathbf{0} = 4\mathbf{g}_f \mathbf{V}_3^1$, $\mathbf{V}_3^1 = \mathbf{0}$ is also gained.

② Using $\frac{d^2\mathbf{q}}{dt_2^2}(1) = \mathbf{\Omega}_2 = 12\gamma_1 (\mathbf{V}_3^1 - \mathbf{V}_2^1) \mathbf{g}_f$, we obtain $\mathbf{V}_2^1 = \mathbf{V}_3^1 - \frac{\text{dexp}^{-1}(\mathbf{V}_3^1) \mathbf{\Omega}_2}{12}$ and $\mathbf{\Omega}_2 = \mathbf{0}$.

③ By the previous result and $\mathbf{q}_1 = \mathbf{g}_{mid} \exp(\mathbf{V}_0^1)$, $\mathbf{q}_3 = \mathbf{g}_f \exp(-\mathbf{V}_3^1)$, and $\mathbf{q}_2 = \mathbf{q}_3 \exp(\mathbf{V}_2^1)$, the second, third and forth vertices of control polygon can be solved.

④ Solving \mathbf{V}_1^2 , \mathbf{V}_0^2 , \mathbf{V}_2^2 by using $\mathbf{V}_1^2 = (1-t)\mathbf{V}_1^1 + t\mathbf{V}_2^1$, $\mathbf{V}_0^2 = (1-t)\mathbf{V}_0^1 + t\mathbf{V}_1^1$, $\mathbf{V}_2^2 = (1-t)\mathbf{V}_2^1 + t\mathbf{V}_3^1$, and substituting solved \mathbf{V}_1^2 , \mathbf{V}_0^2 , \mathbf{V}_2^2 into $\mathbf{V}_0^3 = (1-t)\mathbf{V}_0^2 + t\mathbf{V}_1^2$ and $\mathbf{V}_1^3 = (1-t)\mathbf{V}_1^2 + t\mathbf{V}_2^2$, \mathbf{V}_0^3 , \mathbf{V}_1^3 can also be obtained; by $\mathbf{V}_0^4 = (1-t)\mathbf{V}_0^3 + t\mathbf{V}_1^3$, \mathbf{V}_0^4 can be calculated directly.

⑤ Substituting \mathbf{V}_0^1 , \mathbf{V}_0^2 , \mathbf{V}_0^3 , \mathbf{V}_0^4 into the cumulative equation of the Bezier curve in Lie group $\mathbf{Q}(t) = \prod_{k=4}^1 \exp(t\mathbf{V}_0^k(t)) \mathbf{g}_{mid}$, the curve \mathbf{Q} is obtained.

Step 3 Calculating the second order derivative of \mathbf{Q} in configuration \mathbf{g}_{mid} using $\frac{d^2\mathbf{q}}{dt^2}(0) = 12\gamma_0 (\mathbf{V}_1^1 - \mathbf{V}_0^1) \mathbf{g}_{mid}$, and by application of C^2 continuity condition $\frac{d^2\mathbf{p}}{dt_1^2}(1) = \frac{d^2\mathbf{q}}{dt_2^2}(0)$, the second order derivative of curve \mathbf{P} can also be obtained in junctional configuration.

Step 4 Using the second order derivative of \mathbf{P} and the first derivative in two boundary configurations $\frac{d\mathbf{q}}{dt_1}(0) = \mathbf{0} = 4\mathbf{g}_o \mathbf{V}_0^1$, $\frac{d\mathbf{p}}{dt_1}(1) = \frac{\log(\mathbf{g}_o^{-1} \mathbf{g}_f)}{2} = 4\mathbf{g}_{mid} \mathbf{V}_3^1$, and repeating step 2 and step 3, another Bezier curve \mathbf{P} is solved.

Step 5 Output Bezier \mathbf{P} and \mathbf{Q} , and combine them into one cumulative form.

4 Positioning Path Planning Result Analysis of a Liver Tumor Case

In this paper, based on a liver tumor case, an application example is given to illustrate the solution of positioning path planning. At first the patient's body contour information and tumor boundary information are extracted from CT image. By using CTMRedit described in Ref. [10], all of the image processing and information extraction are completed; CTMRedit segmentation, which uses a seeded region-growing algorithm, is a more suitable method than the snake method to segment an image which has speckle noise and attenuation artifacts. To automatically outline a dark region selected by the user, CTMRedit segmentation's result estimates with an average error of only 0.20 pixels. By CTMRedit the result tumor point set image is shown in Fig.4(a). The corresponding the positioning volume ellipsoid is constructed by the method in section 2.2 and shown in Fig.4(b); the matrix of positioning volume ellipsoid is

$$\mathbf{M} = \begin{bmatrix} 1.0011 & -0.1976 & -0.0227 \\ -0.1976 & 0.7773 & 0.0775 \\ -0.0227 & 0.0775 & 0.05194 \end{bmatrix}$$

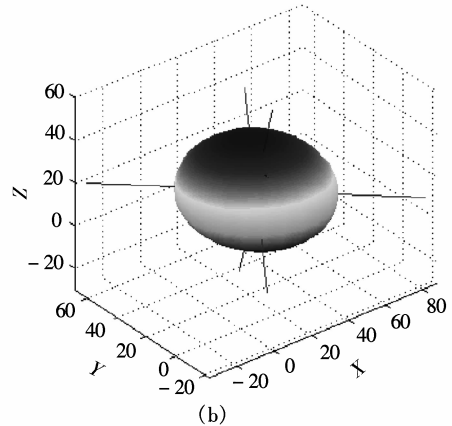
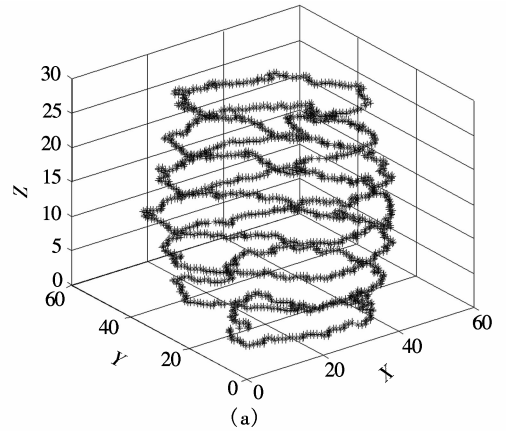


Fig. 4 Tumor contour point set and its positioning volume ellipsoid

and its center is

$$C = \{313.4, 117.1, 468.5\}^T$$

The reconstruction result of the patient's body contour is shown in Fig.5.

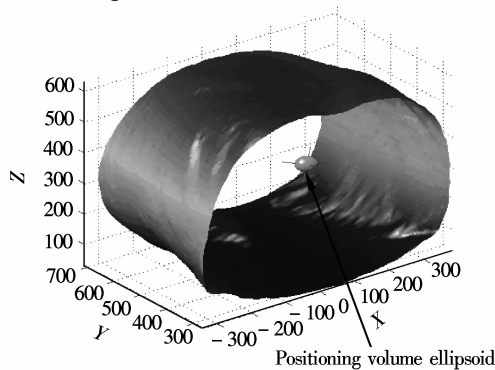


Fig.5 Patient chest and abdomen contour reconstruction result and positioning volume ellipsoid's location in the contour

By application of the method in section 2.3, the selected point set of the patient's body surface enclosed by the specific tetrahedron is presented in Fig.6, where the nearest neighbor search result is indicated by arrow in Fig.6. The coordinate of the closest point is

$$P_k = \{571.2, 181.7, 512.2\}^T$$

After some calculation the result of goal orientation for the positioning motion is

$$\Omega_{\text{goal}} = \{0.1884, 0.1629, 0.2940\}^T$$

Combining these results into configuration, the goal configuration of the positioning motion is $g_f = \{C^T, \Omega_{\text{goal}}^T\}$ and the intermediate configuration is $g_{\text{mid}} = \{P_k^T, 0.8\Omega_{\text{goal}}^T\}$. By some geometrical computation the initial configuration of the platform is $g_o = \{700, 0, 0, 0, 0, 0\}$; all of these three resulting configurations are represented in the coordinate system $X_0Y_0Z_0$.

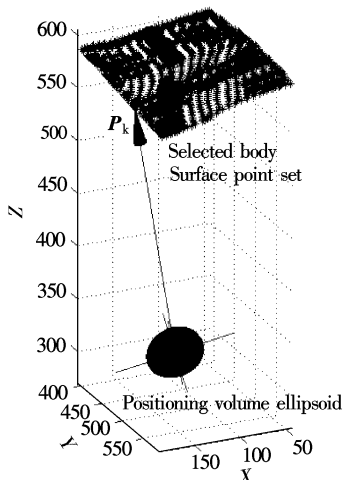


Fig.6 Positioning volume ellipsoid, selected body surface point set and result of nearest neighbor search

The previous three interpolating configurations are used to compute the combined Bezier positioning curve path, and the result is shown in Figs.7 to 10. Fig. 7 indicates planned combined Bezier curve positioning path of C^2 continuity at intermediate configuration, which is represented by the position and orientation transformation of the ultrasound focus ellipsoid in the workspace. Fig.8 shows the spatial curve of the complete planned Bezier positioning path represented by the ultrasound focus ellipsoid's center position transformation in 3-D; the orientation transformation of the ultrasound focus ellipsoid is not presented in the figure. In Fig. 8, the plus sign + represents the general configuration points of the combined Bezier curve path of C^0 continuity at the intermediate configuration, the many of small circles represent general configuration points of the combined Bezier curve path of C^1 continuity at the intermediate configuration; lots of small triangles ∇ represent

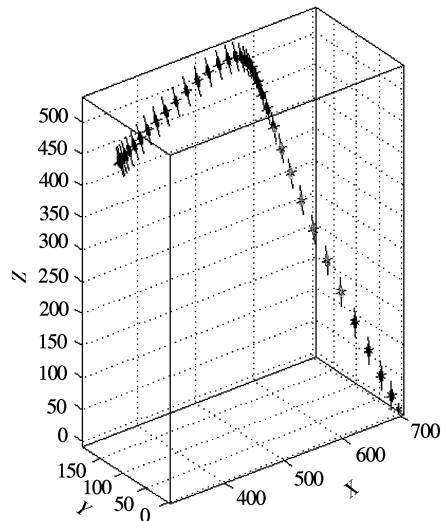


Fig.7 Combined C^2 continuity Bezier curve positioning in workspace

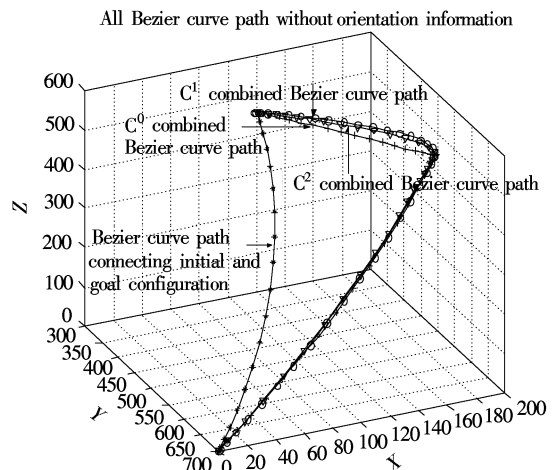


Fig.8 All of planned Bezier positioning path represented by ultrasound focus ellipsoid translation in 3-D

configuration points of the C^2 continuity Bezier curve path. There is another C^2 continuity Bezier curve path in Fig.8, whose configuration points are represented by asterisks *, and by moving along this path, the intermediate configuration determined in the previous computation will not be passed. As shown in Fig.8, the C^0 continuous combined Bezier curve path has an obvious turn at the intermediate configuration, while

the C^1 and C^2 continuity Bezier curve path all have a smooth transition at the intermediate configuration. Figs.9 and 10 present the configuration transformation procedure of different planned Bezier curve paths. Fig. 9 shows the location change of the planned paths, and Fig.10 indicates orientation variation of the planned paths.

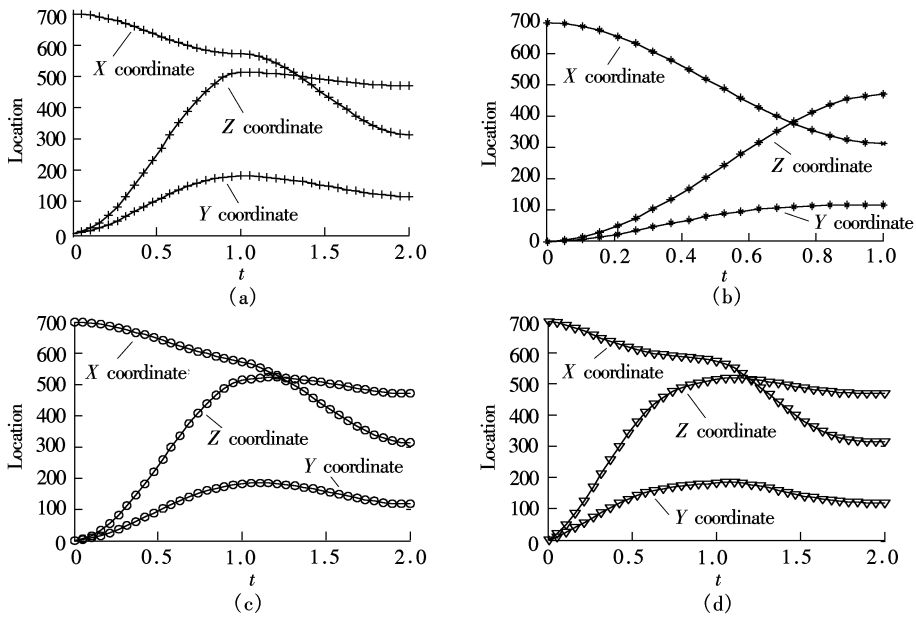


Fig.9 Translation of ultrasound focus ellipsoid in positioning motion along planned different Bezier curve paths. (a) C^0 combined Bezier positioning path; (b) C^2 Bezier path connects initial and goal configuration; (c) C^1 combined Bezier positioning path; (d) C^2 combined Bezier positioning path

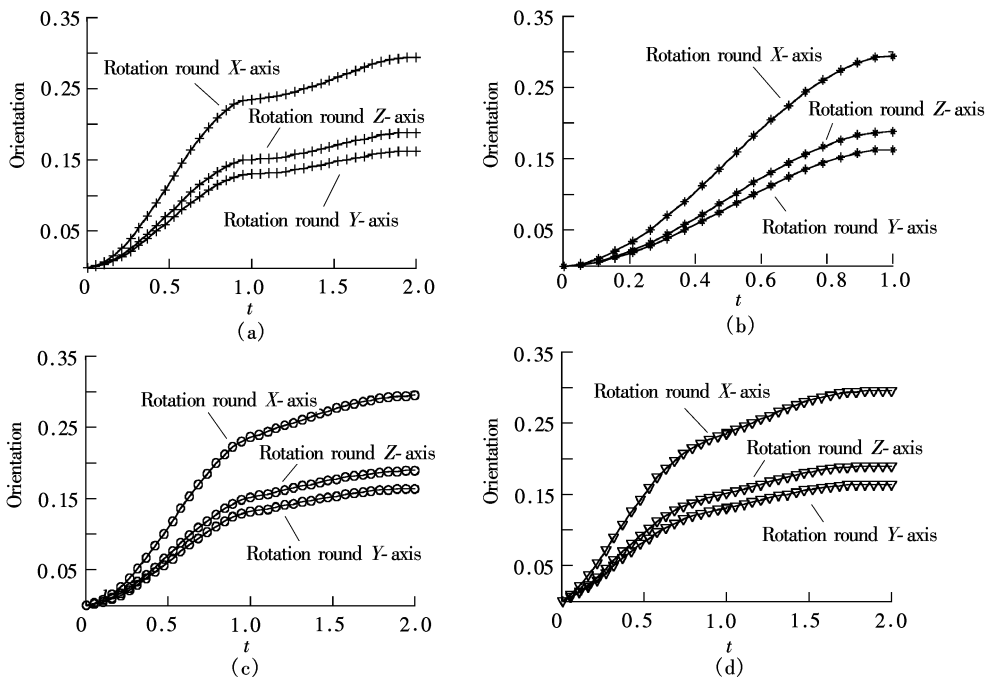


Fig.10 Rotation of ultrasound focus ellipsoid in positioning motion along planned different Bezier curve paths. (a) C^0 combined Bezier positioning path; (b) C^2 Bezier path connects initial and goal configuration; (c) C^1 continuous combined Bezier positioning path; (d) C^2 continuous combined Bezier positioning path

Transformation of each coordinate axis includes translation along the axis and rotation round the axis. As shown in Figs. 9 and 10, the locomotion and rotation transformation curves of each axis have no obvious turn and stagnancy during motion, but according to the second piece of the curves (t changes from 1 to 2), the C^2 continuous combined Bezier curve path is smoother than the C^1 continuity Bezier curve path, which corresponds to Bezier segment $Q(t_2)$. So when positioning along the C^2 continuous combined Bezier curve path, it is held that the treatment head and ultrasound focus ellipsoid can move in a low speed and acceleration during motion corresponds with $Q(t_2)$, and accidental harm to a patient's body resulted from motion is reduced to as low a level as possible.

5 Conclusion

Realization of positioning ultrasound focus ellipsoid to target volume is a prerequisite to using ultrasound focus to treat tumors in the application of the HIFU surgery platform. In this paper, by analysis and planning of the positioning procedure, the fundamental frame for implementation of positioning motion, and the planned C^2 continuous combined Bezier curve path ensure the continuity of the whole positioning motions. Moving along this path the treatment head causes as little unpredictable damage as possible to the patient, so it is a reasonable and feasible path for positioning; in practice by tracking this planned path, the successful positioning to tumor volume can be implemented.

References

[1] Hill C R, Rivens I, Vaughan M G. Lesion development in focused ultrasound surgery: a general model [J]. *Ultrasound Med Biol*, **1994**, **20**(3): 259 – 269.

[2] Davies B L, Chauhan S, Lowe M J. A robotic approach to HIFU based neurosurgery [A]. In: *MICCAI* [C]. Cambridge, 1998. 386 – 396.

[3] Horsch Thomas, Juttler Bert. Cartesian spline interpolation for industrial robot [J]. *Computer Aided Design*, **1998**, **30**(3): 217 – 224.

[4] Crouch Peter, Kun G. The De Casteljau algorithm on Lie group and sphere [J]. *Journal of Dynamical and Control*, **1999**, **15**(3): 397 – 429.

[5] Jouaneh Musa K, Wang Zhixiao, Dornfel David A. Trajectory planning for coordinated motion of a robot and a positioning table — I : path specification [J]. *IEEE Transactions on Robotics and Automation*, **1990**, **6**(6): 735 – 745.

[6] Jiang Xinsong. *An introduction to robotics* [M]. Shenyang: Liaoning Science and Technology Press, 1994. 23 – 87. (in Chinese).

[7] Nene S A, Nayar S K. A simple algorithm for nearest neighbor search in high dimensions [J]. *IEEE Transactions on Pattern Analysis and Machine Intelligence*, **1997**, **19**(9): 989 – 1003.

[8] Murray Richard M, Li Zexiang, Sastry S Shankar. *A mathematical introduction to robotic manipulation* [M]. New York: CPC Press, 1994. 19 – 146.

[9] Piegl Les, Tiller Wayne. *The NURBS book* [M]. Berlin, New York: Springer, 1997. 1 – 34.

[10] Hasegawa-Johnson Mark, Cha Jul Setsu, Haker Katherine. CTMRedit: a Matlab-based tool for segmenting and interpolating MRI and CT images in three orthogonal planes [A]. In: *Proceedings of 1st Joint BMES/EMBS* [C]. Atlanta, GA, USA, 1999. 1170.

高强度聚焦超声手术平台的 Bezier 曲线定位规划

项林清 马培荪 许剑波 高雪官

(上海交通大学机器人研究所, 上海 200030)

摘要: 提出了一种定位区域球方法来表示高强度聚焦超声手术平台在定位运动时肿瘤在其工作空间中的位置和姿态. 针对该简化肿瘤模型, 使用最近邻近查询方法确定了治疗头和超声焦点在定位到肿瘤目标过程中必须经过的中间位姿和目标位姿. 根据确定的位姿, 把组合 Bezier 曲线的连续条件和SO(3)的 De Casteljau 算法结合, 构造出了一条在衔接位姿 C^2 连续的组合 Bezier 曲线路径用于定位, 并且根据一例肝脏肿瘤病例对各种连续路径作了详细分析.

关键词: 定位规划; 工作空间; 关键位姿; 高强度聚焦超声; Bezier 曲线; 连续

中图分类号: TP242.3